The Astrophysical Journal, 597:L57–L60, 2003 November 1

DETECTION OF CLOSE-IN EXTRASOLAR GIANT PLANETS USING THE *FOURIER-KELVIN STELLAR INTERFEROMETER*

William C. Danchi,[1] Drake Deming,[2] Marc J. Kuchner,[3] and Sara Seager[4]
Received 2003 July 16; accepted 2003 September 9; published 2003 October 6

ABSTRACT

We evaluate the direct detection of extrasolar giant planets with a two-aperture nulling infrared interferometer, working at angles $\theta < \lambda/2B$ and using a new "ratio-of-two-wavelengths" technique. Simple arguments suggest that interferometric detection and characterization should be quite possible for planets much closer than the conventional inner working angle, or angular resolution limit. We show that the peak signal from a nulling infrared interferometer of baseline $\lesssim$40 m will often occur "inside the null" and that the signal variations from path difference fluctuations will cancel to first order in the ratio of two wavelengths. Using a new interferometer simulation code, we evaluate the detectability of all the known extrasolar planets as observed using this two-color method with the proposed *Fourier-Kelvin Stellar Interferometer* (*FKSI*). In its minimum configuration *FKSI* uses two 0.5 m apertures on a 12.5 m baseline and a $\pm 20°$ field of regard. We predict that ~7 known extrasolar planets are directly detectable using *FKSI*, with low-resolution spectroscopy ($R \sim 20$) being possible in the most favorable cases. Spaceborne direct detection of extrasolar giant planets is possible with ~12 m baselines and does not require the much longer baselines provided by formation flying.

Subject headings: circumstellar matter — planetary systems — stars: individual (55 Cancri) — techniques: high angular resolution — techniques: interferometric

1. INTRODUCTION

The number of known extrasolar giant planets is now over 100 (Marcy et al. 2003), almost all of which have been detected indirectly, using the radial velocity method. Direct detections of extrasolar giant planets are now becoming possible. For example, Charbonneau et al. (2002) detected the atmosphere of the "transiting planet" HD 209458b using transit spectroscopy (Seager & Sasselov 2000). In the case of planets that do not transit, other techniques of direct detection are being developed, such as visible coronagraphic imaging (Kuchner & Spergel 2003) and nulling infrared (IR) interferometry (Bracewell 1978; Angel & Woolf 1997). A conventional view is that the "inner working angle" (IWA) of a nulling interferometer is the angular distance to the first fringe maximum, i.e., $\lambda/2B$, where B is the interferometer baseline and λ is wavelength. In this Letter, we show that when the likely IR intensities of the extrasolar planets are factored in, nulling IR interferometers having $B \lesssim 40$ m are most sensitive to extrasolar giant planets (EGPs) well inside the conventional IWA, i.e., "inside the null." A substantial number of the known extrasolar planets are directly detectable using interferometry with modest baselines, e.g., the 12.5 m baseline of the minimum configuration of the *Fourier-Kelvin Stellar Interferometer* (*FKSI*) (Danchi et al. 2002, 2003).

2. INTERFEROMETRIC DETECTION "INSIDE THE NULL"?

Simple arguments suggest that interferometric detection can occur for close-in extrasolar giant planets (CEGPs) not fully resolved spatially by the interferometer. First, it is well known that a significant source of noise for a spaceborne nulling interferometer will be photon noise from the leakage of stellar radiation around the "edges" of the null fringe, due to the finite angular radius of the star. If leakage from one stellar radius is a significant noise source, the IR signal from the closest CEGPs, at tens of stellar radii, will also leak through the null fringe. Second, we note that ground-based studies of the CEGPs (Richardson, Deming, & Seager 2003) are beginning to achieve the sensitivity needed to detect the planets in combined light, with no spatial resolution whatsoever.

For a given interferometer baseline, at what angular separation does the transmitted IR signal from an extrasolar planet peak? For decreasing angular separation from the star, the fringe transmission decreases, but the planet's thermal equilibrium temperature in the stellar radiation field increases, so the signal transmitted through the null fringe can remain significant. Distant planets will be observed with fringe transmission of unity, but they will be colder. Figure 1 shows the product of the Planck function at a wavelength of 5 μm times the fringe transmission $[\sin^2(\pi\theta B/\lambda)]$ for baselines of 8, 12, 20, and 40 m. The extrasolar system was assumed to be at 10 pc distance, and the planet was assumed to emit as a blackbody in thermal equilibrium with a Bond albedo of 0.4. These "interferometer contribution functions" were normalized to unity for the peak signal at the 40 m baseline. The asterisks on each curve mark the nominal IWA at $\lambda/2B$.

Figure 1 shows that even for the longest (40 m) baseline, the peak signal occurs inside the nominal IWA at $\lambda/2B$. For the shorter baselines, the peak occurs quite far inside the IWA. For example, the 12 m peak signal occurs for planets near 0.1 AU, a factor of 4 below $\lambda/2B$. For all baselines, the decrease in signal at the greatest distances occurs because of the lower planetary temperatures. Although the peak signal for the 12 m baseline occurs near 0.1 AU, this signal is reduced by about an order of magnitude from the 40 m case. Figure 1 suggests that the sensitivity of a 12 m interferometer working "inside the null" may be sufficient to allow detection and characterization of some of the known extrasolar giant planets.

[1] NASA Goddard Space Flight Center, Infrared Astrophysics Branch, Code 685, Greenbelt, MD 20771; William.C.Danchi@nasa.gov.
[2] NASA Goddard Space Flight Center, Planetary Systems Branch, Code 693, Greenbelt, MD 20771; ddeming@pop600.gsfc.nasa.gov.
[3] Hubble Fellow, Department of Astrophysical Sciences, Princeton University, Princeton, NJ 08544; mkuchner@astro.princeton.edu.
[4] Department of Terrestrial Magnetism, Carnegie Institution of Washington, Washington, DC 20015; seager@dtm.ciw.edu.

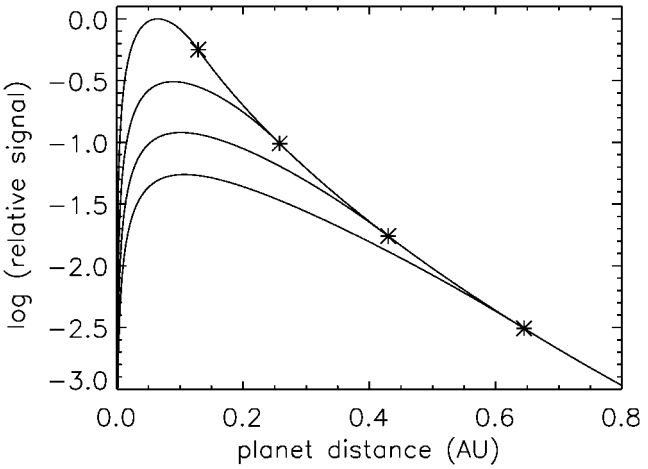

FIG. 1.—Log of the peak planetary signal seen at $\lambda = 5$ μm by a nulling interferometer of baseline 40, 20, 12, and 8 m (*upper to lower curves*). The asterisks mark the nominal inner working angles at $\lambda/2B$. The curves were normalized to unity for the peak signal at the 40 m baseline. The IR intensity of the planet was computed from blackbody equilibrium, with Bond albedo 0.4 and distance 10 pc.

3. A TWO-COLOR METHOD

Using a simple analytical model of the nulling interferometer we demonstrate that the ratio of the intensity at the output of the nuller at two wavelengths is insensitive to the residual path length fluctuations, provided they are small compared to the wavelength. A nulling interferometer operates like a conventional stellar interferometer except that an achromatic π phase shift is applied to the beam coming from one element of the interferometer and that the beams are symmetrically and achromatically combined. The equation for the normalized intensity, $N(\lambda_1)$, is

$$N(\lambda_1) = \frac{1}{2}[1 - |V(\lambda_1)| \cos \phi(\lambda_1)], \tag{1}$$

where λ_1 is the first wavelength, $|V(\lambda_1)|$ is the modulus of the visibility of the source, and $\phi(\lambda_1) = 2\pi\sigma_N/\lambda_1$ is the rms phase error caused by residual path length fluctuations, σ_N, in the system. For a point source and no path length fluctuations, equation (1) reduces to the usual θ^2 null of the classical Bracewell interferometer. A similar equation holds for the output of the same nuller at a second wavelength, λ_2. Using these assumptions,

$$|V(\lambda_1)| \approx 1 - \frac{\pi^2}{16}\left(\frac{\theta_{\rm star}}{\lambda_1/B}\right)^2, \tag{2}$$

where $\theta_{\rm star}$ is the angular diameter of the star and B is the baseline length, and similarly expanding the term for the phase fluctuations,

$$\cos \phi(\lambda_1) \approx 1 - \frac{\phi(\lambda_1)^2}{2} = 1 - 2\pi^2\left(\frac{\sigma_N}{\lambda_1}\right)^2. \tag{3}$$

Substituting these equations into equation (1) and using similar equations for the second wavelength, λ_2, it is easy to show that

$$\frac{N(\lambda_1)}{N(\lambda_2)} \approx \left(\frac{\lambda_2}{\lambda_1}\right)^2. \tag{4}$$

Hence the stellar leakage and path length fluctuations cancel out.

This result is valid for the case when the interferometer is not rotating about the line of sight or when the residual path length fluctuations occur at much higher frequencies than the rotation frequency about the line of sight. The cancellation occurs in the leakage signal variations that accompany instability in the null fringe (not in the photon noise) and that would otherwise overwhelm the planetary signal. This technique is expected to work best when the two wavelengths λ_1 and λ_2 are reasonably close together, avoiding higher order effects.

TABLE 1

NOMINAL PARAMETERS FOR *FKSI*

Parameter	Value
Baseline	12.5 m
Aperture	2 × 0.5 m diameter
Field of regard	±20°
Efficiency	0.05 (electrons out/photons in)
Spectral resolution	$\lambda/\delta\lambda = 20$
Path length stability	15 nm rms; 10 s time constant
Wavelength range	3 μm ≤ λ ≤ 8 μm
Optics temperature	63 K
Detector temperature	35 K
Dark current	0.2 e^- s^{-1}
Read noise	8 e^-

4. AN INTERFEROMETER SIMULATION CODE

We have written a simulation code to compute the signal from the known extrasolar giant planets, as observed by a rotating two-aperture nulling interferometer, following the principle of Bracewell (1978) and treating the output signal as a ratio, exploiting the rationale given above.

The code uses the interferometer parameters for *FKSI* as listed in Table 1. The modeled fringe pattern of the interferometer includes path difference errors, based on the current *FKSI* error budget. Shot noise is computed from the total signal, including the stellar leakage, the extrasolar zodiacal background, and the instrument thermal background. Dark current and read noise from the detection system are also included. The stellar spectrum is assumed to be a blackbody, but wavelength-dependent limb darkening is imposed on the disk, based on the solar observations of Pierce et al. (1950). The stellar temperature and radius are estimated from the spectral type. The planet is modeled as a blackbody spectrum with superposed molecular band spectral structure. The planet's blackbody equilibrium temperature is computed assuming a Bond albedo of 0.4; the planetary radius is taken to be 35% greater than that of Jupiter, based on HD 209458b (Brown et al. 2001). The planetary spectral structure was included by interpolating in the "cloudless" sequence computed by Sudarsky, Burrows, & Hubeny (2003). The planetary spectrum is currently assumed to be independent of orbital phase and inclination to the line of sight. Orbital motion of the planet is included, using orbital elements from the Doppler observations and a nominal inclination of 45°. The zodiacal background is calculated including

contributions from both scattered light and thermal radiation.[5] Since younger stars will have more massive zodiacal disks, we scaled the mass of the disk as the -1.76 power of the stellar age (Spangler et al. 2001). Ages for stars hosting extrasolar planets were taken from Laws et al. (2003). The inclination of the zodiacal disk is also included (nominally 45° to the plane of the sky), since the asymmetry from the inclined disk produces a significant signal as the interferometer rotates.

5. EXAMPLE OF AN *FKSI* DETECTION

We have simulated observations by *FKSI* of all known extrasolar planetary systems using the code. An example is shown in Figure 2, which illustrates the detection of 55 Cancri b. Figure 2*a* shows the number of photons detected versus wavelength, at the *FKSI* spectral resolving power ($\lambda/\delta\lambda = 20$), in one 300 s integration. The calculated wavelength range in Figure 2 extends longward of the nominal wavelength limits of *FKSI*. The dominant source of photons is stellar leakage, with planetary radiation second. The zodiacal radiation falls below the planetary intensity for this old and dust-poor system (Jayawardhana et al. 2002). The dominant source of noise depends on wavelength but is due to stellar leakage shot noise at the shortest wavelengths, thermal background radiation noise at the longest wavelength (>8 μm), and dark current and read noise at intermediate wavelengths. Since the anticipated total integration time during an observational "campaign" for a given planetary system can be many days, planets whose photon counts fall well below the noise level in a single 300 s integration will nevertheless be detectable. But for 55 Cancri b, the planetary signal photon counts are comparable to the noise photons in a single 300 s integration, for wavelengths longer than 3 μm. This planet is strongly detectable, and more extensive spectral information could also be extracted.

In the original Bracewell concept, the rotation of the interferometer modulates the planetary signal, and we have included this process in the simulation code. Figure 2*b* (*lower panel*) shows a power spectrum from a signal time series of 55 Cancri b. As per our two-color method, the Fourier-transformed signal in this case was the intensity integrated over wavelengths $6\ \mu\mathrm{m} \geq \lambda \geq 3\ \mu\mathrm{m}$, ratioed to the intensity integrated over $\lambda < 3\ \mu$m. The denominator in this ratio is dominated by the stellar leakage at the shortest wavelengths and contains minimal planetary signal. The planet peaks at the longer wavelengths in the numerator. The greater null depth at long wavelengths enhances this separation of planet and stellar signals.

The interferometer was rotated slowly, about 15 hours per rotation, and the simulated campaign lasted about 35 days (50 rotations). The zodiacal signal appears in the Figure 2*b* power spectrum at twice the interferometer rotation frequency, i.e., at 37 μHz, and the planetary signal also contributes at this frequency. Because of the planet's orbital motion, the planetary signal appears primarily at a different frequency (see legend), slightly displaced, and *resolved* from the zodiacal signal. Moreover, because the planet is inside the null, no overtones are caused by transmission through higher order fringes. Note also that as the signal from the planet goes in and out of phase with the zodiacal signal, the envelope of this modulation is seen in the low-frequency region of the power spectrum as a peak at 1.6 μHz, twice the orbital frequency of the planet.

[5] M. J. Kuchner 2002, IDL software program ZODIPIC (http://cfa-www.harvard.edu/~mkuchner).

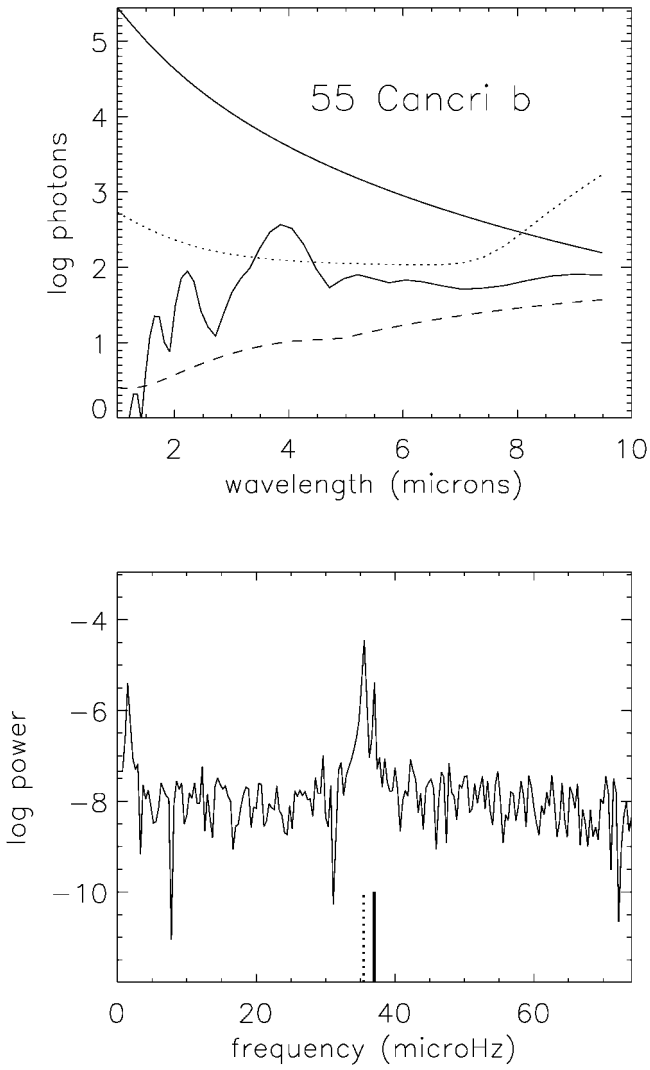

FIG. 2.—Simulated observations of the innermost planet in the 55 Cancri system ($a = 0.11$ AU, $P = 14.65$ days) using *FKSI*. The upper panel (Fig. 2*a*) shows the number of photons detected at a single interferometer rotation angle (where the planet signal is maximum), in a 300 s integration. The stellar leakage is the upper solid line, and the detected planetary spectrum is the lower solid line. The dashed line is the zodiacal component, and the dotted line is the total noise. The lower panel (Fig. 2*b*) shows the power spectrum from a simulated 35 day observing campaign (50 rotations of the interferometer). The marks on the frequency axis indicate $2\nu_i$ (*solid mark*) and $2|\nu_i - \nu_p|$ (*dashed mark*), where ν_i is the rotation frequency of the interferometer and $\nu_p = 1/P$, where P is the orbital period of the planet.

6. DISCUSSION

Our simulations show that a significant number of known extrasolar planets will be detectable using *FKSI* and that spectral information can be derived in several of the most favorable cases. These simulated detections are robust in the sense that the few most favorable planetary systems are detectable with almost any reasonable instrumental configuration (baseline, aperture size, etc.) or choice of long-wavelength cutoff. However, detections for the fainter systems depend significantly on the instrumental parameters and wavelength range, as well as on the properties of the detectors (dark current, read noise).

Figure 3 illustrates the distances and orbital semimajor axes

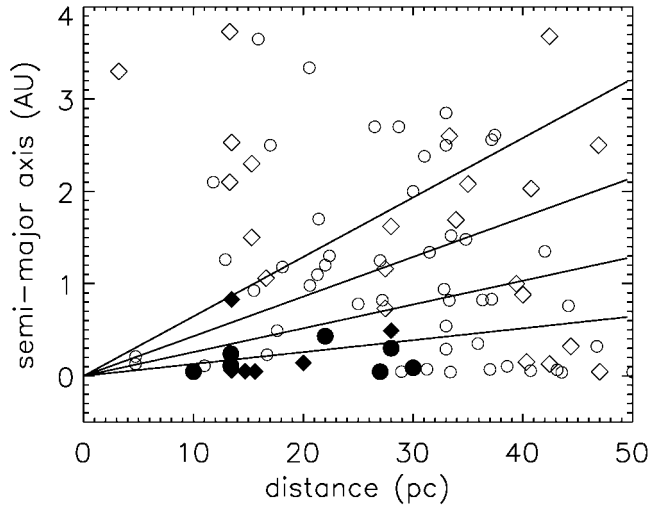

FIG. 3.—Distance (pc) and orbital radius (semimajor axes, in AU) of known extrasolar planets (having $d \leq 50$ pc and $r \leq 4$ AU and within a $\pm 40°$ field of regard). The planets nominally detectable by *FKSI* are plotted with filled symbols; circles indicate planets within a $\pm 20°$ field of regard, and diamonds indicate additional detectable planets if the field of regard is extended to $\pm 40°$. The lines correspond to the first fringe maximum for nulling interferometers of baselines 8, 12, 20, and 40 m (*top to bottom*), at $\lambda = 5$ μm.

for many of the known planetary systems, with those systems detectable by *FKSI* (using Table 1 parameters) plotted as filled symbols. The $\pm 20°$ field of regard holds seven detectable planets, and an additional six planets are within a $\pm 40°$ field of regard. The conventional IWA resolutions for baselines of 40, 20, 12, and 8 m are overplotted. It can be seen that the detectable planets are essentially the CEGP systems closest to Earth, with essentially no dependence on the angular resolution limits (IWA lines).

Our results show that planets can be detected much closer to stars than expected based on the concept of the inner working angle, computed from the nominal resolution of the interferometer, i.e., $\lambda/2B$. This resolution estimate is essentially the same as the Rayleigh criterion for conventional telescopes, which is the angular separation of two stars of equal intensity in which one star is placed at the first zero of the Airy pattern of the second star. The Rayleigh criterion is well known to be a very conservative estimate of resolution, and sources can be resolved that are substantially closer than this, using superresolution techniques such as the pixon method (Pina & Puetter 1993). Similar considerations hold for interferometers as CLEAN, MEM, and other methods have provided images with effective angular resolutions much better than nominally expected (Cobb & Fix 1987).

For a wavelength of 5 μm, the resolution of the *FKSI* is $\lambda/2B \approx 41$ milliarcseconds (mas). But our simulations demonstrate an "effective resolution" of approximately 1 mas. Our results are consistent with the working resolution of the interferometer being determined by the ratio of the rms path length fluctuation to the baseline, σ_N/B, which for the parameters in this paper is 0.2 mas. This is not as surprising as it may seem at first, since the path length stability requirement to achieve a 10^{-4} null or better is essentially that of an interferometer with extremely high phase stability.

The work presented here has important implications for the *Terrestrial Planet Finder* mission (Beichman, Woolf, & Lindensmith 1999), because angular resolution is often emphasized over sensitivity. The desire for a nulling interferometer using free-flyer telescopes is based on the resolution needed to search more than 150 F, G, and K stars for Earth-like planets in the habitable zone (J. I. Lunine et al. 2003, TPF Science Working Group, unpublished). Given that the actual IWA can be significantly smaller than previously thought means that it may be possible to achieve the basic goals of TPF with a structurally connected interferometer having a modest baseline in the range of 20–30 m.

We thank R. Allen, D. Benford, D. Gezari, D. Leisawitz, J. Monnier, M. Mumma, L. Mundy, C. Noecker, and W. Traub for their contributions to the *FKSI* mission concept.

REFERENCES

Angel, J. R. P., & Woolf, N. J. 1997, ApJ, 475, 373
Beichman, C., Woolf, N. J., & Lindensmith, C., eds. 1999, A NASA Origins Program to Search for Extrasolar Planets (JPL Publ. 99-3; Pasadena: JPL)
Bracewell, R. N. 1978, Nature, 274, 780
Brown, T. M., Charbonneau, D., Gilliland, R. L., Noyes, R. W., & Burrows, A. 2001, ApJ, 552, 699
Charbonneau, D., Brown, T. M., Noyes, R. W., & Gilliland, R. L. 2002, ApJ, 568, 377
Cobb, M. L., & Fix, J. D. 1987, ApJ, 315, 325
Danchi, W. C., et al. 2002, AAS Meeting, 201, 51.09
———. 2003, in Towards Other Earths, ed. B. Battrick (ESA SP-539; Noordwijk: ESA), in press
Jayawardhana, R., Holland, W. S., Kalas, P., Greaves, J. S., Dent, W. R. F., Wyatt, M. C., & Marcy, G. W. 2002, ApJ, 570, L93
Kuchner, M. J., & Spergel, D. 2003, in ASP Conf. Ser. 294, Scientific Frontiers in Research on Extrasolar Planets, ed. D. Deming & S. Seager (San Francisco: ASP), 603
Laws, C., Gonzalez, G., Walker, K. M., Tyagi, S., Dodsworth, J., Snider, K., & Suntzeff, N. B. 2003, AJ, 125, 2664
Marcy, G. W., Butler, R. P., Fischer, D. A., & Vogt, S. S. 2003, in ASP Conf. Ser. 294, Scientific Frontiers in Research on Extrasolar Planets, ed. D. Deming & S. Seager (San Francisco: ASP), 1
Pierce, A. K., McMath, R. R., Goldberg, L., & Mohler, O. C. 1950, ApJ, 112, 289
Pina, R. K., & Puetter, R. C. 1993, PASP, 105, 630
Richardson, L. J., Deming, D., & Seager, S. 2003, ApJ, 597, 581
Seager, S., & Sasselov, D. D. 2000, ApJ, 537, 916
Spangler, C., Sargent, A. I., Silverstone, M. D., Becklin, E. E., & Zuckerman, B. 2001, ApJ, 555, 932
Sudarsky, D., Burrows, A., & Hubeny, I. 2003, ApJ, 588, 1121